Covenant Journal of Physical & Life Sciences (CJPL) Vol. 9 No. 2, December 2021
ISSN: *print 2354 - 3574 electronics 2354 – 3485* DOI:

An Open Access Journal Available Online

Thermo-Diffusion Effects of a Stagnation Point Flow in a Nanofluid with Convection using the Adomian Decomposition Method

Abdulhakeem Yusuf[1]*, Mohammed Ilyasu Gupa[1], Nana Hauwa Sayeed[2], and Gbolahan Bolarin [1]

[1]Mathematics Department, Federal University of Technology, PMB 65, Minna, 00176-0000 Nigeria, Niger State, Nigeria

[2] Department of Mathematics, Faculty of Science, Air Force Institute of Technology, Kaduna, Kaduna State

*Corresponding author: aust_royal@yahoo.co.uk

Received: 09.05.2021; Accepted: 02.02.2022
Date of Publication: December 2021

***Abstract*:** The Thermo-diffusion solution effects a stagnation point flow of a nanofluid with convection using. Adomian Decomposition Method (ADM) is presented. The Partial differential equation representing the problem was reduced to an ordinary differential equation by introducing some similarity transformation variables. The transformed equations were solved using the ADM and the results were compared with existing results in the literatures. There is a good agreement between the method and the existing one, which indicate reliability of the method. The physical parameters that occurred in the solutions such as magnetic parameter, thermal Grashof numbers, concentration Grashof numbers, nano Lewis number, velocity ratio, Prandtl number were varied to determine their respective effects. It was observed that when the wall velocity is higher than the free stream velocity $\left(A \prec 1\right)$, the fluid velocity drop and rises when velocity at free stream is higher than the wall velocity $\left(A \succ 1\right)$.

Keywords: Adomian decomposition method, Nanofluid, Nanoparticles, Solutal concentration, Velocity ratio, Grashof number.

1.0 Introduction

Crane [1] analyses the problem of stagnation point flow near a solid surface. Immediately the study was concluded, many other researchers went into the flow of boundary layers incorporating several other parameters [2, 3].

Works on fluids conducted electrically are very important due to their applicability in modern metallurgy and metalworking processes. Nanofluids with incorporated magnetic fields are used to control the flow and heat transfer by regulating the velocity of the fluid. Mahapatra and Gupta [4] Examine the stagnation point flow of

MHD over a stretching sheet via numerical simulations. The stagnation point flow of a magnetohydrodynamic nanofluid was depicted by [5] using the classical Runge-Kutta method. Several other analyses on MHD nanofluid are presented in [6, 7] and references therein. Choi *et al.*[8] presented a study that depicted that the conventional fluids thermal conductivity can be increased by adding nanoparticles to the base fluid, which also incorporate some other thermal properties. In electronic cooling, double plane windows, heat exchanger. These new enhancements can be seen practically. Buongiorno [9] showed a comprehensive nanotechnology-based fluid model that depicted thermal properties' advantages over base fluid. A better and more encompassing model was developed, and nanofluid's convective properties were fully discussed. After all these developments in nanofluid, the boundary layer flow over a stretching sheet was first studied by [10] using the model of [11, 12]. Mehta and Kataria [17] presented a study of heat generation/absorption effect on unsteady natural convective MHD second-grade fluid flow past an oscillating vertical plane in the presence of thermal radiation and chemical reaction. They found out that heat generation increases the fluid temperature, increasing the fluid velocity. More extensive works as contained in the works of [18], [19], [20], [21].

Nanofluid is an improved heat transfer medium, having nanoparticles (1–100 nm) that are stably and uniformly distributed in a base fluid. These distributed nanoparticles, generally a metal or metal oxide, greatly enhance the nanofluid's thermal conductivity, increasing conduction and convection coefficients, allowing for more heat transfer [13].

This study is a new advancement in the literature in which the analytical study of thermo-diffusion effects of a stagnation point flow of a nanofluid with convection is presented. The main objectives are to obtain the problem's solution at all points using the Adomian decomposition method to present the effects of all the physical parameters that appear in the solutions to the flow.

Generally, this work consists of 5 different sections in which section I is the general introduction of the work. Section II present the problem formulation, section III presents the methodology employed to obtain the solutions, section IV describes the results and their respective discussion and section V is the conclusion.

2.0 Materials and Methods

2.1 Problem Formulation

Considering an incompressible 2-dimensional Magnetohydrodynamic stagnation point flow of a nanofluid towards a stretching sheet with wall temperature T_W, solutal concentration C_W, nanoparticle concentration φ_w , and larger values of the stretching sheet, respectively. Following the formulation in [14] with natural convection, the governing equations for continuity, momentum, temperature, solutal and nanoparticle concentrations are written as follows:

$$\frac{\partial u}{\partial x}+\frac{\partial v}{\partial y}=0 \qquad (1)$$

$$\left(u\frac{\partial u}{\partial x}+v\frac{\partial u}{\partial y}\right)=U_{\infty}\frac{\partial U_{\infty}}{\partial x}+$$
$$\upsilon\left(\frac{\partial^2 u}{\partial x^2}+\frac{\partial^2 u}{\partial y^2}\right)+\frac{\sigma B_0^2}{\rho}\left(U_{\infty}-u\right) \quad (2)$$
$$+g\beta\left(T-T_{\infty}\right)+$$
$$g\beta\left(C-C_{\infty}\right)$$

$$\left(u\frac{\partial T}{\partial x}+v\frac{\partial T}{\partial y}\right)=\alpha_m\left(\frac{\partial^2 T}{\partial x^2}+\frac{\partial^2 T}{\partial y^2}\right)+$$
$$\tau\begin{bmatrix} D_T\left(\frac{\partial\varphi\partial T}{\partial x\partial x}+\frac{\partial\varphi\partial T}{\partial y\partial y}\right)+ \\ \frac{D_T}{T_{\infty}}\left(\frac{\partial T}{\partial x}+\frac{\partial T}{\partial y}\right)^2 \end{bmatrix}+ \quad (3)$$
$$D_{TC}\left(\frac{\partial^2 C}{\partial x^2}+\frac{\partial^2 C}{\partial y^2}\right)$$

$$\left(u\frac{\partial C}{\partial x}+v\frac{\partial C}{\partial y}\right)=D_S\left(\frac{\partial^2 C}{\partial x^2}+\frac{\partial^2 C}{\partial y^2}\right)+$$
$$D_{CT}\left(\frac{\partial^2 T}{\partial x^2}+\frac{\partial^2 T}{\partial y^2}\right) \quad (4)$$

$$\left(u\frac{\partial \varphi}{\partial x}+v\frac{\partial \varphi}{\partial y}\right)=D_B\left(\frac{\partial^2 \varphi}{\partial x^2}+\frac{\partial^2 \varphi}{\partial y^2}\right)+$$
$$\frac{D_T}{T_{\infty}}\left(\frac{\partial^2 T}{\partial x^2}+\frac{\partial^2 T}{\partial y^2}\right) \quad (5)$$

Subject to the boundary condition:

$$\left.\begin{array}{l} u=U_w=ax,\;\; v=0, \\ T=T_w,\; C=C_w, \\ \varphi=\varphi_w \;\; y=0 \\ u=U_{\infty}=bx,\; T=T_{\infty}, \\ C=C_{\infty},\; \varphi=\varphi_{\infty} \;\; y\to\infty \end{array}\right\} \quad (6)$$

Where velocity along x and y axes are u and v respectively, ρ is the density of the base fluid, υ is the kinematic viscosity, σ is the electrical conductivity, α_m is the heat diffusivity, K_T is the heat-distribution ratio, g acceleration due to gravity, β volumetric coefficient of thermal expansion, D_{TC} is the Duffour diffusivity, B_0 external magnetic field, D_{CT} is the Soret Diffusivity, C_p is the specific heat capacity at constant pressure, D_B is the Brownian diffusion coefficient, D_T is the thermospheric diffusion coefficient and $\tau=\frac{(\rho c)_p}{(\rho c)_f}$ is the ratio between the effective heat capacity of the fluid with D_s as the solutal diffusivity, U_w and U_{∞} are the wall velocity and free stream velocity respectively.

In other to reduce (1) - (6) into ODEs, the following similarity transformational variables are defined as follows:

$$\eta=\sqrt{\frac{a}{\upsilon}}y,\;\; u=axf^{/}\left(\eta\right),$$
$$v=-\sqrt{a\upsilon}\,f\left(\eta\right),\theta=\frac{T-T_{\infty}}{T_w-T_{\infty}},$$
$$s=\frac{C-C_{\infty}}{C_w-C_{\infty}},\phi=\frac{\varphi-\varphi_{\infty}}{\varphi_w-\varphi_{\infty}}$$
(7)

where η, $f\left(\eta\right)$, $\theta\left(\eta\right)$, $s\left(\eta\right)$ $\phi\left(\eta\right)$ are the dimensionless fluid distance, velocity, temperature, solutal and nanoparticle concentrations.

From (7), we have the following transformation:

$$\eta = \sqrt{\frac{a}{\upsilon}}y, u = axf^{/}, v = -\sqrt{a\upsilon}f(\eta)$$
$$\frac{\partial u}{\partial y} = \frac{\partial u}{\partial \eta}\frac{\partial \eta}{\partial y} = axf^{//}\sqrt{\frac{a}{\upsilon}} \quad (8)$$

Introducing equation (8) into equations (1) to (6), the PDEs reduces to

$$\left.\begin{aligned}
&f^{///} + ff^{//} - f^{/2} + A^2 \\
&+M\left(A - f^{/}\right) \\
&+G_{rT}\theta + G_{rC}s = 0 \\
&\theta^{//} + P_r f\theta^{/} + P_r N_b \theta^{/}\phi^{/} \\
&+P_r N_t \theta^{/2} + P_r Nds^{//} = 0 \\
&s^{//} + 2Lefs^{/} \\
&+Ld\theta^{//} \\
&\phi^{//} + Lnf\phi^{/} \\
&+\frac{N_t}{N_b}\theta^{//} = 0 \\
&f(0) = 0, f^{/}(0) = 1, \\
&\theta(0) = 1, s(0) = 1, \phi(0) = 1 \\
&f^{/}(\infty) = A, \theta(\infty) = 0, \\
&s(\infty) = 0, \phi(\infty) = 0
\end{aligned}\right\} \quad (9)$$

where

$$M=\frac{\sigma B_0^2}{ax\rho}, G_{rT}=\frac{g\beta\left(T_w-T_\infty\right)}{a^2x\upsilon},$$

$$G_{rC}=\frac{g\beta\left(C_w-C_\infty\right)}{a^2x\upsilon}$$

$$A=\frac{b}{a}, P_r=\frac{\upsilon}{\alpha_m}, \mathrm{N}_b=\frac{\tau D_T\left(\varphi_w-\varphi_\infty\right)}{\upsilon},$$

$$\mathrm{N}_t=\frac{\tau D_T}{\upsilon T_\infty}\left(T_w-T_\infty\right),$$

$$Nd=\frac{D_{TC}\left(C_w-C_\infty\right)}{\upsilon\left(T_w-T_\infty\right)}$$

$$Le=\frac{\upsilon}{D_s}, Ld=\frac{D_{CT}\left(T_w-T_\infty\right)}{\left(C_w-C_\infty\right)},$$

$$Ln=\frac{\upsilon}{D_B}$$

are magnetic parameter, thermal Grashof number, solutal concentration Grashof number, velocity ratio, Prandtl number, Brownian motion, thermophoresis parameter, modified Dufour parameter, Lewis number, Dufour solutal Lewis number, nano Lewis number.

2.2 Methodology

The method of ADM is employed to obtain the solution of problem (9) by letting

$\frac{d^3}{d\eta^3}=L_1$ and $\frac{d^2}{d\eta^2}=L_2$ and from the problem (9), we have

$$\left.\begin{aligned}
&f^{///}=-ff^{//}+f^{/2}-M\left(A-f^{/}\right)\\
&-A^2-G_{rT}\theta-G_{rC}s\\
&\theta^{//}=-P_r f\theta^{/}-P_rN_b\theta^{/}\phi^{/}-\\
&P_rN_t\theta^{/2}-Nds^{//}\\
&s^{//}=-Lefs^{/}-Ld\theta^{//}\\
&\phi^{//}=-Lnf\phi^{/}-\frac{N_t}{N_b}\theta^{//}
\end{aligned}\right\} \quad (10)$$

Introducing the operators into (10) we have

$$\left.\begin{aligned}
&L_1^{-1}L_1\left[f\left(\eta\right)\right]\\
&=L_1^{-1}\begin{bmatrix}-ff^{//}-A^2-M\left(A-f^{/}\right)\\ -G_{rT}\theta-G_{rC}s\end{bmatrix}\\
&L_2^{-1}L_2\left[\theta\left(\eta\right)\right]=\\
&L_2^{-1}\begin{bmatrix}-P_r f\theta^{/}-P_rN_b\theta^{/}\phi^{/}-\\ P_rN_t\theta^{/2}-Nds^{//}\end{bmatrix}\\
&L_2^{-1}L_2\left[s\left(\eta\right)\right]\\
&=L_2^{-1}\left[-Lefs^{/}-Ld\theta^{//}\right]\\
&L_2^{-1}L_2\left[\phi\left(\eta\right)\right]\\
&=L_2^{-1}\left[-Lnf\phi^{/}-\frac{N_t}{N_b}\theta^{//}\right]
\end{aligned}\right\} \quad (11)$$

Introducing the polynomials in [15] into (11), we have

$$\left.\begin{aligned}
&\sum_{n=0}^{\infty} f_n = -L_1^{-1}\sum_{n=0}^{\infty} A_n + \\
&L_1^{-1}\sum_{n=0}^{\infty} B_n - ML_1^{-1}\sum_{n=0}^{\infty}\left(A - f_n^{/}\right) \\
&-G_{rT}L_1^{-1}\sum_{n=0}^{\infty}\theta_n - G_{rC}L_1^{-1}\sum_{n=0}^{\infty} s_n - A^2 \\
&\sum_{n=0}^{\infty}\theta_n = -P_r L_2^{-1}\sum_{n=0}^{\infty} C_n - \\
&P_r N_b L_2^{-1}\sum_{n=0}^{\infty} D_n - P_r N_t L_2^{-1}\sum_{n=0}^{\infty} E_n \\
&-NdL_2^{-1}\sum_{n=0}^{\infty} s_n^{//} \\
&\sum_{n=0}^{\infty} s_n = -LeL_2^{-1}\sum_{n=0}^{\infty} F_n - LdL_2^{-1}\sum_{n=0}^{\infty}\theta^{//}{}_n \\
&\sum_{n=0}^{\infty}\phi_n = -LnL_2^{-1}\sum_{n=0}^{\infty} G_n - \frac{N_t}{N_b}L_2^{-1}\sum_{n=0}^{\infty}\theta_n^{//} \\
&where\ A_n = f_n f_{n-k}^{//}, B_n = f_n^{/} f_{n-k}^{/}, \\
&\mathrm{C}_n = f_n\theta_{n-k}^{/}, D_n = \theta_n^{/}\phi_{n-k}^{/},\ \mathrm{E}_n = \theta_n^{/}\theta_{n-k}^{/} \\
&F_n = f_n s_{n-k}^{/}, G_n = f\phi_{n-k}^{/}
\end{aligned}\right\}$$

(12)

$$\left.\begin{aligned}
&f_{n+1} = -L_1^{-1}\sum_{k=0}^{n} f_n f_{n-k}^{//} + \\
&L_1^{-1}\sum_{k=0}^{n} f_n^{/} f_{n-k}^{/} + ML_1^{-1} f_n^{/} \\
&-G_{rT}L_1^{-1}\theta_n - G_{rC}L_1^{-1}s_n \\
&\theta_{n+1} = -P_r L_2^{-1}\sum_{k=0}^{n} f_n\theta_{n-k}^{/} - \\
&P_r N_b L_2^{-1}\sum_{k=0}^{n}\theta_n^{/}\phi_{n-k}^{/} - \\
&P_r N_t L_2^{-1}\sum_{k=0}^{n}\theta_n^{/}\theta_{n-k}^{/} - NdL_2^{-1}s_n^{//} \\
&s_{n+1} = -LeL_2^{-1}\sum_{k=0}^{n} f_n s_{n-k}^{/} \\
&-LdL_2^{-1}\theta_n^{//} \\
&\phi_{n+1} = -LnL_2^{-1}\sum_{k=0}^{n} f_n\phi_{n-k}^{/} \\
&-\frac{N_t}{N_b}L_2^{-1}\theta_n^{//}
\end{aligned}\right\}$$

(13)

Where
$$\left.\begin{aligned} f_0(\eta) &= \eta + \frac{\alpha_1 \eta^2}{2} - \\ &\left(MA + A^2\right)\frac{\eta^3}{6} \\ \theta_0(\eta) &= 1 + \eta\alpha_2 \\ s_0(\eta) &= 1 + \eta\alpha_3 \\ \phi_0(\eta) &= 1 + \eta\alpha_4 \end{aligned}\right\} \tag{14}$$

are the initial guesses.

3.0 Results

The results obtained from section 3 above are presented and discussed in this section. Maple 16 software was used to compute the integrals and also to plot the graphical solutions presented in this section Table 1 and Table 2 show the validation of the present method with the existing method in the literature. A good agreement is observed among these methods. The slight difference results from the analytical method employed, which gives results at all points.

Figure 1 shows the effect of the velocity ratio on the velocity profile. It is an observer that when the free stream velocity is lower than the stretching sheet (A=0.8, 0.4), the velocity drops below 1 and rises above when otherwise (A= 2.8, 2.1, 1.4) [14]. Figure 2 shows the effects of the thermal Grashof number on the velocity profile. As the Grashof number increases, the velocity also increases due to the possessed's buoyancy effect.

Figure 3 shows the effects of solutal grashof number on the velocity profile. It is observed that as the solutal Grashof number is enhancing, the velocity profile is also increasing. Figure 4 is the variation of the magnetic parameter on the velocity profile, and it is observed that as the magnetic parameter increases, the velocity profile reduces due to the drag like force present in the magnetic field [20]. Figures 5 to 6 shows the effects of Prandtl number on temperature and nanoparticle concentration profiles. As the Prandtl number increases, the temperature of the fluid reduces while the nanoparticle concentration is enhancing [14].

Figures 7 to 8 are the graphs of Brownian motion parameters on the fluid temperature and nanoparticle concentration profiles. It is seen that as the Brownian motion parameter increases, both fluid temperature and nanoparticle concentration also increase.

Figures 9 to 10 are the graphs of thermophoresis parameters on the fluid temperature and nanoparticle concentration profiles. It is seen that as the thermophoresis parameter increases, both fluid temperature and nanoparticle concentration also increase [13]. Figures 11 to 13 display the effects of modified Dufour number on the fluid temperature solutal and nanoparticle concentrations, respectively. As the modified Dufour number increases, the temperature and the solutal concentration increase while the nanoparticle concentration profile is a reduction agent. Figure 14 show the effects of Lewis number on solutal concentration profile, and it is observed that as the Lewis number increases, solutal concentration profile reduces. Figure 15 show the effects of nano Lewis number on nanoparticle concentration profile, and it is observed that as the Lewis number increases, nanoparticle concentration profile reduces [14]. Figure 16 presents the Dufour solutal Lewis number variation on the solutal concentration profile. As the Dufour solutal Lewis number increases, the solutal concentration profile also thickens [14].

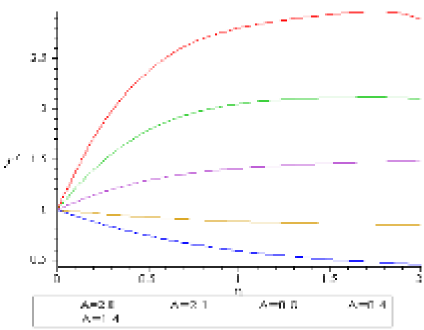

Figure 1: Variation of velocity ratio on velocity

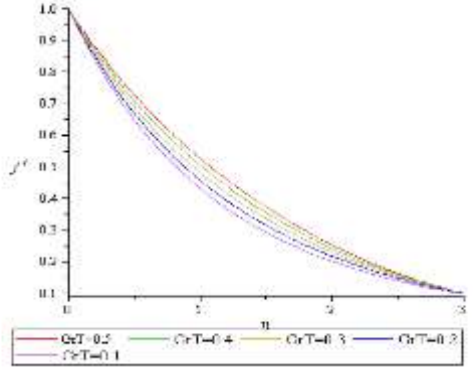

Figure 2: Variation of thermal Grashof number on velocity

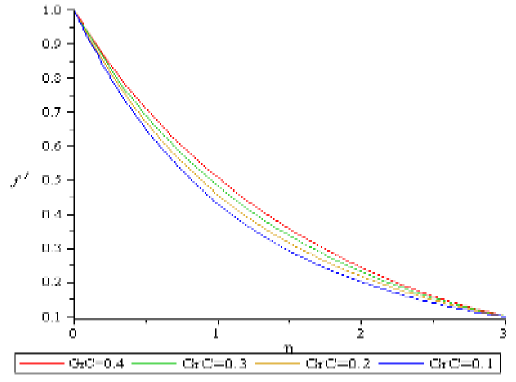

Figure 3: Variation of concentration Grashof number on velocity

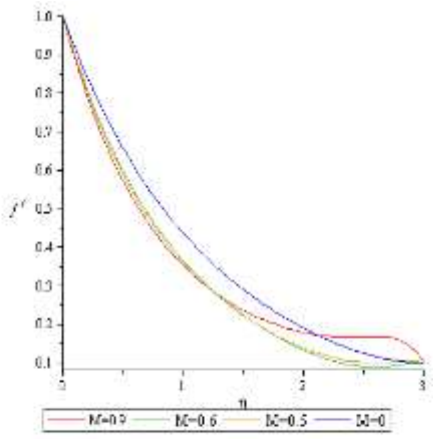

Figure 4: Variation of magnetic parameter on velocity

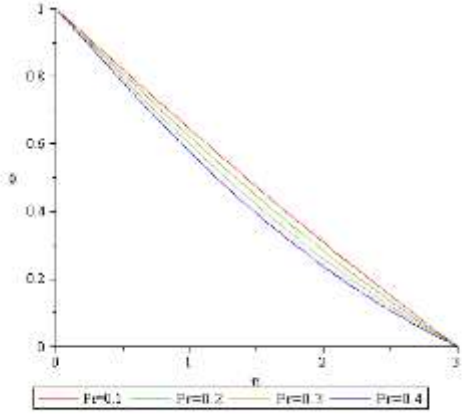

Figure 5: Variation of Prandtl number on temperature

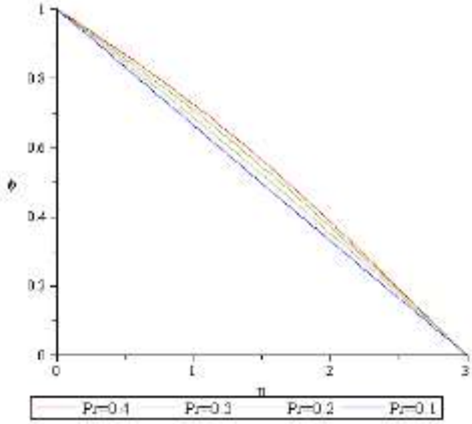

Figure 6: Variation of Prandtl number on nanoparticle

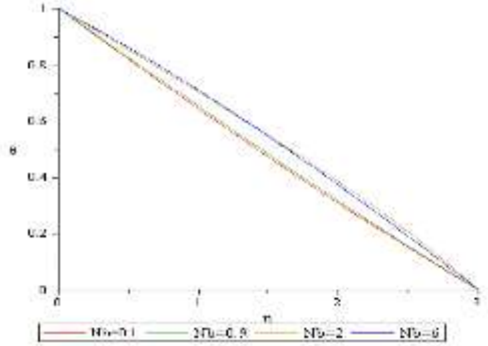

Figure 7: Variation of Brownian motion on temperature

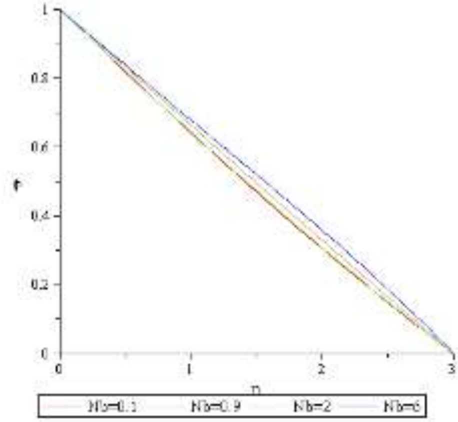

Figure 8: Variation of Brownian motion on nanoparticle

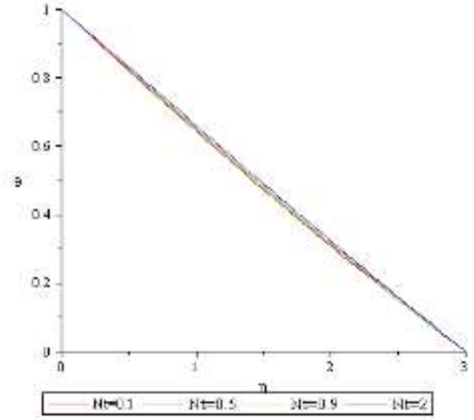

Figure 9: Thermopherosis parameter on temperature

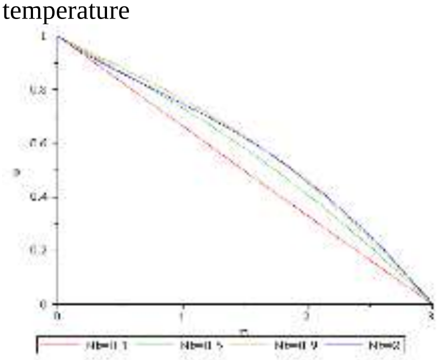

Figure 10: Thermopherosis parameter on nanoparticle

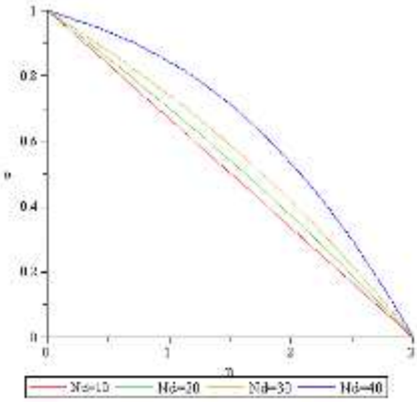

Figure 11: Modify Dufour parameter on temperature

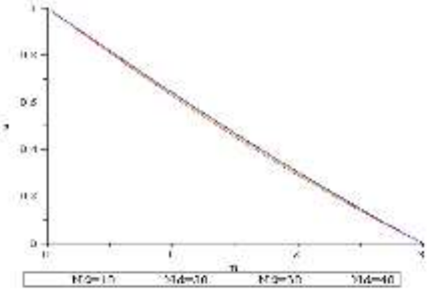

Figure 12: Modify Dufour parameter on solutal

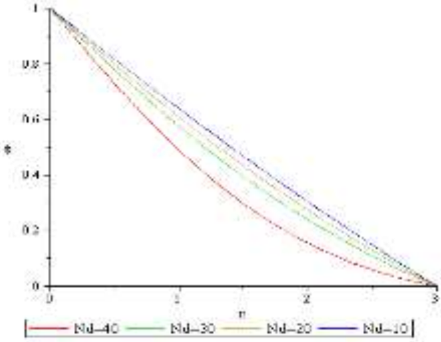

Figure 13: Modify Dufour parameter on nanoparticle

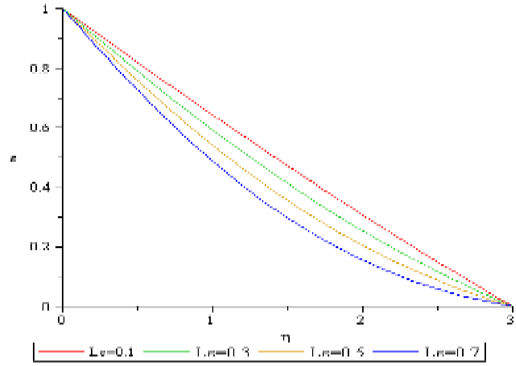

Figure 14: Lewis number on solutal concentration

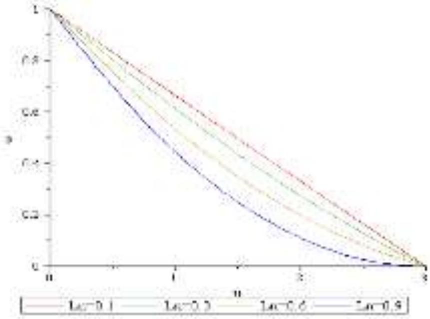

Figure 15: Nano Lewis number on nanoparticle

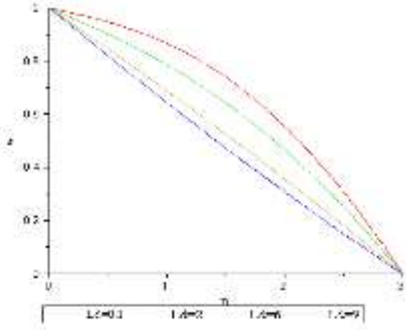

Figure16: Dufour solutal Lewis number on solutal

Table 1: Comparison of values of $f^{//}(0)$ with existing solutions for $M = G_{rC} = G_{rT} = 0$

A	Present Results	[14]	[5]	[16]
0.01	-	-0.998	-0.998	-0.998
	-0.9774	-	-	-
0.1		0.9694	0.9694	0.9694
	-0.9206	-	-	-
0.2		0.9181	0.9181	0.9181
	-0.6608	-	-	-
0.5		0.6673	0.6673	0.6673
2	2.0223	2.0175	2.0175	2.0175

Table 2: Comparison of values for local Nusselt number $-\theta^{/}(0)$ with existing solutions for $N_b = N_t = Nd = 0$

Pr	A	Present Results	[16]	[12]	[15]
1	0.1	0.6329	0.6021	0.6022	0.603
1	0.3	0.6564	0.6244	0.6255	0.625
1	0.5	0.6856	0.6924	0.6924	0.692
1.5	0.1	0.6965	0.7768	0.7768	0.777
1.5	0.3	0.7412	0.7971	0.7971	0.797
1.5	0.5	0.8124	0.8647	0.8648	0.863

5.0 Conclusion

This work extends the work of [14] by introducing the buoyancy effects. The problem was presented in its rectangular form and later reduced to nonlinear coupled ordinary differential equations. The method of [15] was used to solve the problem, and results are validated with [14], [16], [5]. The main findings are:

i. A good agreement was established between the present method and the comparison.

ii. The physical parameters that occurred in the solutions, such as Grashof numbers, enhanced the velocity profile.

iii. Prandtl number is found to lower the fluid temperature.

Finally, this work can be extended further by incorporating additional parameters into the model. Another method, be it analytical or numerical, can also be employed to obtain the solution of the new extension.

6.0 References

[1] Crane, L. J. (1970). Flow past a stretching plate, Zeitschrift für angewandte Mathematik und Physik ZAMP 21 (4), 645–647.

[2] W.H.H. Banks, W. H. H. (1983). Similarity solutions of the boundary layer equations for a stretching wall, Journal de Mecanique Theorique et Appliquee 2, 375–392.

[3] Kazem, S., Shaban, M., Abbasbandy, S. (2011). Improved analytical solutions to a stagnation-point flow past a porous stretching sheet with heat generation, Journal of the Franklin Institute 348, 2044–2058.

[4] Mahapatra, T. R., Gupta, A. G. (2002). Heat transfer in stagnation mpoint flow towards a stretching sheet, Heat Mass Transfer 38, 517–521.

[5] Ibrahim, W., Shankar, B., Nandeppanavar, M. M. (2013). MHD stagnation point flow and heat transfer due to nanofluid towards a stretching sheet, International Journal of Heat and Mass Transfer 56, 1–9.

[6] Zeeshan, A., Ellahi, R., Siddiqui, A. M., Rahman, H. U. (2012). An investigation of porosity and magnetohydrodynamic flow of non-Newtonian nanofluid in coaxial cylinders, International Journal of Physical Sciences 7 (9), 1353–1361.

[7] Kuznetsov, A. V., Nield, D. A. (2011). Double-diffusive natural convective boundary layer flow of a nanofluid past a vertical plate, International Journal of Thermal Sciences 50 (5), 712–717.

[8] Choi, S. U. S., Zhang, Z. G., Yu, W., Lockwood, F. E., Grulke, E. A. (2001) Anomalously thermal conductivity enhancement in nanotube suspensions, Applied Physics Letters 79, 2252–2254.

[9] Buongiorno, J. (2006). Convective transport in nanofluids, ASME Journal of Heat Transfer 128 (2006) 240–250.

[10] Khan, W. A., Pop, I. (2010) Boundary-layer flow of a nanofluid past a stretching sheet, International, Journal of Heat and Mass Transfer 53, 2477–2483.

[11] Nield, D. A., Kuznetsov, A. V. (2009). The Cheng-Minkowycz problem for natural convective boundary-layer flow in a porous medium saturated by nanofluid, International Journal of Heat and Mass Transfer 52, 5792–5795.

[12] Kuznetsov, A. V., Nield, D. A. (2009). Natural convective boundarylayer flow of a nanofluid past a vertical plate, International Journal of Thermal Sciences 49 (2) (2009) 243–247.

[13] Yusuf, A., Bolarin, G., Jiya, M., Aiyisimi, Y.M. (2018). Boundary layer flow of a nanofluid in an inclined wavy wall with convective boundary condition. Comm. Maths Mod and Appl, 3, 48-56

[14] Khan, U., Ahmad, N., Khan, S. I. U., Mohyud-din, S. T. (2014). Thermo-diffusion effects on MHD stagnation point flow towards a stretching sheet in a nanofluid. Propulsion and Power Research http://dx.doi.org/10.1016/j.jppr.2020.04.01.

[15] Adomian, G. (1994) Solving frontier problem of Physics: The Decomposition method. Springer-Science +Business 6.

[16] Mustafaa, M., Hayat, T., Pop, I., Asghar, S., Obaidat, S. (2011). Stagnation-point flow of a nanofluid towards a stretching sheet. International Journal of Heat and Mass Transfer, 54, 5588–5594.

[17] Mehta, R., Kataria, H. R. (2020) Magnetic field a heat generation effect on second grade fluid flow past an Oscillating vertical plate in porous medium, International Journal of scientific Research in Mathematical and Statiscal Sciences, 7(2), 01-08 .

[18] Sheikholeslami, M., Bhatti, M. M. (2017). Active method for nanofluid heat transfer enhancement by means of EHD International Journal of Heat Mass Transfer, 109, 115–122.

[19] Mishra, S. R., Bhatti, M. M. (2017) Simultaneous effects of chemical reaction and Ohmic heating with heat and mass transfer over a stretching surface: a numerical study, Chin. Journal of

Chemical Engineering, 5.

[20] Bhatti, M. M., Ali Abbas, M., Rashidi, M. M. (2018) A robust numerical method for solving stagnation point flow over a permeable shrinking sheet under the influence of MHD. Journal of Applied Mathematics and Computation, 316, 381-389.

[21] Bolarin, G., Yusuf, A. Emmanuel, O., and Aiyesimi, Y. M. (2019). Magnetohydrodynamics (MHD) flow of a third grade fluid through a cylindrical pipe in an inclined plane with radiation. Covenant Journal of Physical and life Sciences (CJPL), 7 (1), June, ISSN, 2354-3574e. 2354-3485 DOI:10.20370/v09m-vp86.